Bounded phase phenomena in the optically injected laser

B. Kelleher,[1,2] D. Goulding,[2,3] B. Baselga Pascual,[1,2] S. P. Hegarty,[2] and G. Huyet[1,2]
[1]*Centre for Applied Photonics and Process Analysis, Cork Institute of Technology, Cork, Ireland*
[2]*Tyndall National Institute, Lee Maltings, Cork, Ireland*
[3]*Department of Physics, University College Cork, Cork, Ireland*

(Received 16 November 2011; revised manuscript received 3 February 2012; published 18 April 2012)

Two routes to phase-locking in the optically injected laser system are investigated both involving limit cycles where the phase of the slave laser is unlocked but is nevertheless bounded. We use an experimental phase-resolving technique to unambiguously demonstrate the phenomenon via explicit phasors for the slave laser electric field. Theoretical considerations show that for locking mechanisms involving Hopf bifurcations, such limit cycles of bounded phase are generic. For weakly damped devices, such as quantum well lasers, this can involve an excited resonance at the relaxation oscillation frequency. For highly damped devices there is no such excitation but the bounded phase behavior must persist. Phasor portraits for other regimes are also obtained including a chaotic regime.

DOI: 10.1103/PhysRevE.85.046212 PACS number(s): 05.45.Xt, 42.60.Mi, 42.55.Px, 42.65.Sf

I. INTRODUCTION

The optically injected laser provides an excellent test-bed for coupled oscillators in general and for synchronization phenomena in particular. Many interesting nonlinear dynamical regimes can be observed in the system and while certain features are generic, the details can differ depending on the type of slave laser in question. Conventional Class B (quantum well and bulk) lasers are treated extensively in Ref. [1] and references within; quantum dot lasers are considered in Refs. [2,3] and comparisons with quantum well lasers are described in Ref. [4]; optically injected Class A lasers are treated in Ref. [5]. Inherently bistable lasers have also attracted considerable attention with studies of dynamics in optically injected vertical-cavity surface-emitting lasers [6–8], semiconductor ring lasers [9], and two-mode Fabry Pérot lasers [10].

The relaxation oscillations (ROs) of a semiconductor laser describe the underdamped oscillator-like response to perturbations from steady-state operation. For certain parameter ranges under optical injection, the ROs of conventional semiconductor lasers can be excited and become self-sustained. As the injection strength is varied there are three possibilities. The first is that the injected field may be too weak to excite the resonance; in this case the locking bifurcation is a saddle-node bifurcation, and the physics of the system is similar to the Adler model [11]. Generalizations of the Adler model may be required to accurately model the behavior [12,13] but the principle is the same. The second possibility is to have the injection strength in the right range so that the resonance can be excited. In this case, the locking bifurcation is of Hopf form, and the frequency of the limit cycle created in the bifurcation is approximately that of the ROs. Once the locking mechanism is a Hopf bifurcation, any approximation using the Adler model is fundamentally flawed. The third possibility is that the injection strength is too high to excite the RO resonance. The locking mechanism is still of Hopf form, but there is never a limit cycle at the RO frequency. We show below that this last case is of particular interest for highly damped devices.

There are also three possible generic behaviors for the phase of the slave laser. It is possible for the master laser to phase lock the slave in which case the frequency of the slave matches that of the master and the phase is fixed relative to that of the master. The second is found when the laser is neither frequency locked nor phase locked and the phase of the slave is unbounded (for example, far from the locking region where the operation approximates frequency beating between the two lasers). The third case is where the slave is not phase locked to the master but in some sense its average frequency is still that of the master. In this case the phase of the slave varies but is bounded both above and below. This regime was originally recognized in Refs. [14,15] and elsewhere since. As we show below, the phase operation just outside the locking boundary is deeply related to the type of bifurcation that produces the locking. When the locking is via saddle node, then the phase can be unbounded until locking is obtained just as in the Adler model. However, if the locking is via Hopf, then one should expect the bounded phase behavior.

The phenomenon of varying but bounded phase behavior is by no means limited to the optically injected laser, but the laser system is one that lends itself well to experimental analysis and the phenomenon was recently demonstrated in Ref. [16]. In this work we demonstrate the phenomenon via direct measurements of bounded phase limit cycles using the phase-resolving technique described in Ref. [17]. This phasor technique allows a more complete analysis and description of the dynamics than can be obtained using only the conventional spectral and intensity measurements. We show explicit experimental phasors for two routes to unlocking through a bounded phase regime. The first results from a quantum well device and involves the resonance related to the ROs. A chaotic regime is also investigated. The appearance of chaos is typical at low injection strengths for weakly damped devices and often appears as an intermediate regime between the RO related bounded-phase limit cycle and the detuning related unbounded-phase limit cycle. The second route we examine is for a highly damped quantum dot device at a high injection level where the bounded phase regime is not associated with any intrinsic frequency in the device. There is no intermediate regime between the bounded and unbounded cycles; rather the bounded cycle simply grows and migrates in the electric field plane becoming unbounded when it surrounds the origin. This route is typical of highly damped and Class A devices and even weakly damped devices at high injection levels.

II. RATE EQUATION MODEL

The conventional Class B [18] semiconductor laser rate equations are

$$\dot{R} = NR + K\,\cos\phi, \tag{1}$$

$$\dot{\phi} = -\Delta + \alpha N - \frac{K}{R}\,\sin\phi, \tag{2}$$

$$\dot{N} = \gamma[P - N - (1+2N)\,R^2]. \tag{3}$$

Here a dot means differentiation with respect to T, where $T = t/t_{\mathrm{ph}}$ is time measured in units of the photon lifetime t_{ph}, R is the slave field amplitude, ϕ is the phase of the slave minus that of the master, N is the carrier density of the slave, K is the injection rate, Δ is the detuning (the frequency of the master minus that of the slave), α is the linewidth enhancement factor of the slave laser, γ is the ratio of the photon lifetime to the carrier lifetime, and P gives the pumping current above threshold. (In the phasor figures throughout this work, the real part of the slave electric field $R\cos\phi$ is denoted by E_R and the imaginary part of the slave electric field $R\sin\phi$ is denoted by E_I.)

By linearizing Eqs. (1)–(3), one can find the characteristic equation which is of third order in this system [19]. From this we find an expression for the frequency Ω_H of the limit cycle created in the Hopf bifurcation:

$$\Omega_H^2 = 2\gamma P + \eta^2 - 4\gamma N\left(\frac{1+P+N}{1+2N}\right). \tag{4}$$

Here $\eta \equiv \frac{K}{R}$, and N and η both take their steady state values at the Hopf bifurcation parameters in question. There are three separate terms: the first is the square of the free-running RO frequency, the second is an injection induced term, and the third is a combination of RO properties and injection terms (through injection induced changes in N). This expression allows us to easily find some general results about the frequency of the Hopf bifurcation. First let us consider the well-known (but still instructive) case of weak damping and weak injection [20]. From these assumptions one finds easily that at a Hopf bifurcation, the frequency of the resulting limit cycle is given by $\Omega_H^2 \approx 2\gamma P = \Omega_{\mathrm{RO}}^2$. That is, the Hopf frequency is that of the free-running ROs. This result is of course already very well known. It is strictly a low injection level result. Let us consider now weak damping but high injection levels.

In this case the Hopf bifurcation no longer results in sustained oscillations at approximately the free-running RO frequency. This is quite clear by examining Eq. (4). As the injection strength is increased, the second term in Eq. (4) can become greater than the other two and so, for weak damping and sufficiently high injection levels $\Omega_H \approx \eta$. Of course, the Hopf bifurcation still results in sustained oscillations, but the value of the frequency for these oscillations is no longer approximated by the free-running RO frequency. Using the steady state solutions we find two further expressions that will allow us to find Ω_H in terms of the detuning. Firstly, the steady state value of N is bounded, satisfying

$$-\tfrac{1}{2} < N \leqslant P. \tag{5}$$

Secondly, the trigonometric identity $\cos^2\phi + \sin^2\phi = 1$ can be used to find

$$\eta^2 = \Delta^2 - 2\alpha\Delta N + (1+\alpha^2)N^2. \tag{6}$$

Since N is bounded we have that for sufficiently high injection levels $\eta^2 \approx \Delta^2$ and so $\Omega_H^2 \approx \Delta^2$ from Eq. (4). That is, the Hopf frequency for high injection levels is given to leading order by the absolute value of the detuning (a fact previously recognized in Ref. [21]).

Nonetheless, the route to locking must still involve a bounded phase limit cycle. That this must be so can be shown as follows. The phase-locked point results from the collapse of the limit cycle in the Hopf bifurcation. If the cycle always surrounds the origin, then the locked point would have to be the origin and so the intensity of the slave would be zero. This is manifestly not the case and so the cycle must be of bounded phase prior to locking. This high injection level behavior will be of great relevance below when we consider highly damped slave lasers.

Note that if the locking bifurcation is of saddle-node form, then no such restriction applies. In this case there are two typical scenarios. The fixed points can be born on a limit cycle of unbounded phase as in the Adler locking scenario. Alternatively, the fixed points can be born away from the limit cycle, and the phase-locked solution can coexist with the limit cycle until the cycle is destroyed in a homoclinic bifurcation [12,22]. In both cases the cycle can remain one of unbounded phase.

III. EXPERIMENTAL QUANTUM WELL PHASORS

The experimental setup used the interferometric system introduced in Ref. [17] and since used in Ref. [12] to investigate the phase behavior of optically injected semiconductor lasers. The master laser was a commercial tunable laser with a linewidth of approximately 100 kHz. The slave laser was a single (discrete) mode quantum well based device (Eblana Photonics) emitting at approximately 1.3 μm. The phase of the slave laser in the frame of the master was measured, and Fig. 1 shows time series plots of the slave laser intensity and the associated phasor plots. In Figs. 1(a) and 1(b) the intensity and phasor of a phase-locked point at a detuning of approximately −0.68 GHz are shown. The detuning was increased until at a value of approximately 0.9 GHz the slave unlocked via a Hopf bifurcation producing an oscillating output of frequency 6.4 GHz, close to the RO frequency of the free-running device. As the detuning was further increased the intensity oscillations became more pronounced, and the intensity and the associated phasor of such a cycle are shown in Figs. 1(c) and 1(d), respectively. The detuning at this point was approximately 2 GHz. The origin is quite clearly outside the cycle providing a definitive, unambiguous example of a bounded limit cycle.

By increasing the detuning even further the behavior became chaotic, a regime of interest to many researchers (see [23] and references therein). An example of the intensity and the associated phasor in this regime are shown in Fig. 2. In the intensity trace we see pulsations of varying height with no obvious underlying pattern. There is a strong influence on the trace from the ROs; the time between successive pulsations in many cases is close to the RO period. The phasor plot shows the underlying phase trajectories and there are two notable

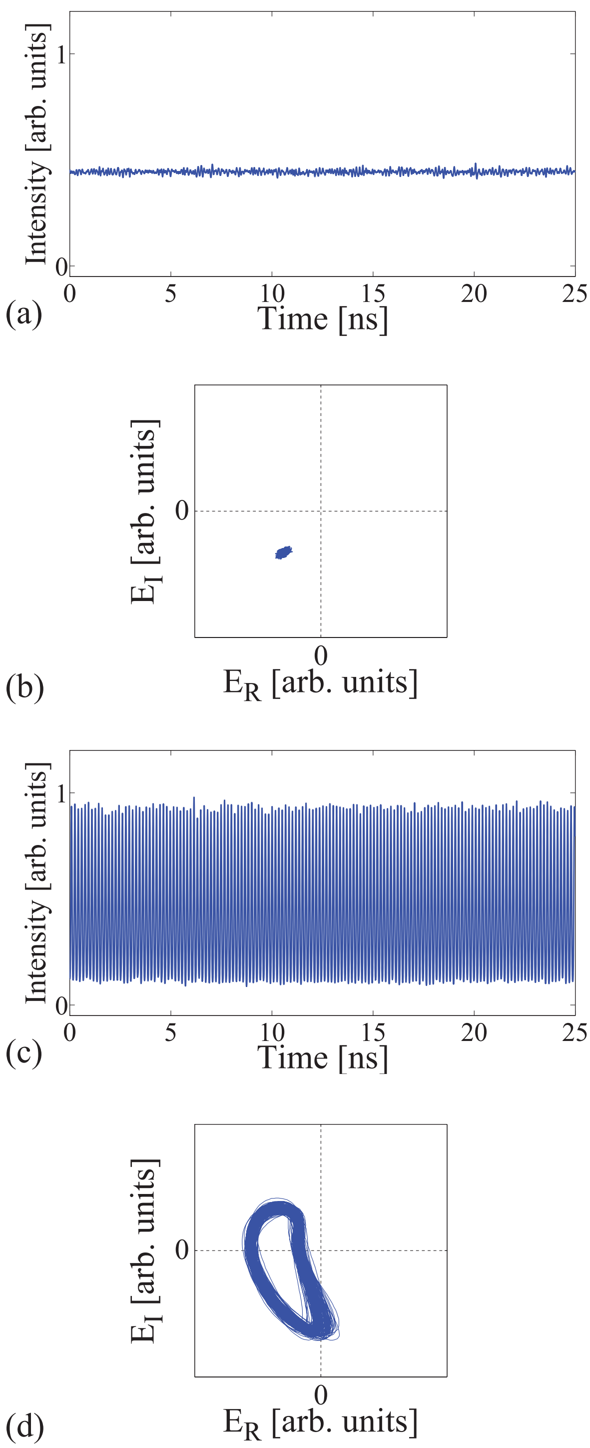

FIG. 1. (Color online) Experimental intenisty and associated phasor traces. The device was operated at approximately 1.5 times threshold current. (a), (b) Phase-locked behavior with fixed phase (modulo noise) at a detuning of approximately -0.68 GHz. (c), (d) Unlocked behavior with bounded phase at a detuning of approximately 2 GHz.

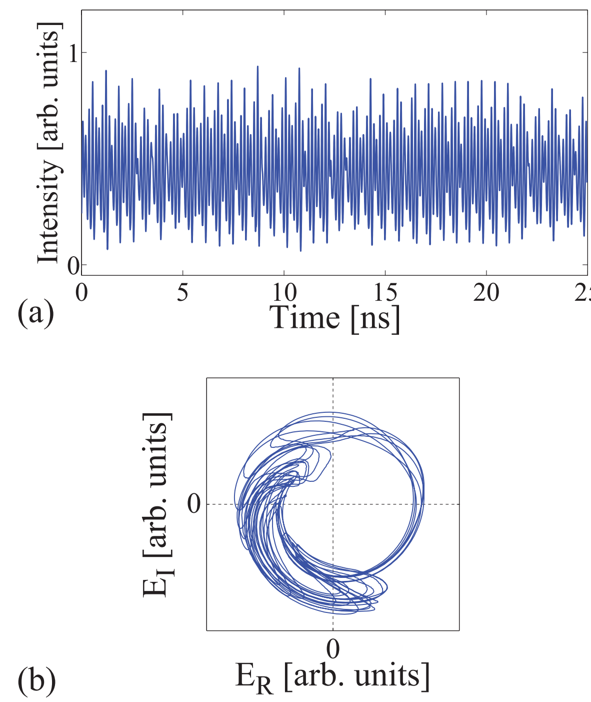

FIG. 2. (Color online) Experimental intensity and associated phasor traces for a chaotic regime at a detuning of approximately 3.4 GHz.

features. The first is that the phase is now unbounded as the trajectory surrounds the origin. The second is that there appear to be two components to the trajectory. One is the large "unbounded" component on the right of Fig. 2(b) and the other is the crowded "bounded" region on the left of the figure. The bounded component results from the weakly damped ROs and produces the smaller pulsations in the intensity, while the unbounded component produces the large pulsations and will develop into an unbounded limit cycle at large detunings [17]. The phasor shows quite clearly the combination of the influences of both the unbounded behavior prevalent at large detunings and the bounded behavior prevalent closer to the locking region.

IV. HIGHER DAMPING: THEORY

We considered earlier the effect of increasing the injection strength using Eq. (4) and showed that the association of the Hopf bifurcation with RO undamping ceased to be valid. We consider now an increase in the damping. This has a similar effect. The first consideration is the effect on the location of the codimension 2 intersection of the saddle-node and Hopf bifurcations. In Ref. [19] it was shown that for weak damping the detuning at this point is proportional to γ. At low injection levels this means that the injection strength at the codimension 2 point is also proportional to γ, and so as the damping is increased, the codimension 2 point moves to ever higher injection levels. This codimension 2 point is the point at which the Hopf bifurcation becomes stable. Thus, as this point moves to ever higher injection strengths, eventually there is no longer a stable Hopf bifurcation at low injection levels and so the physical interpretation of undamped ROs no longer holds since the weak injection approximation is no longer valid. Instead, there is a mixture of injection and RO terms involved in the Hopf frequency. As the damping becomes very high in the Class A limit [18] there are of course no ROs at all, and yet there is still a Hopf bifurcation and so for a Class B laser with sufficiently high γ the Hopf bifurcation must be (at least approximately) independent of any RO phenomena. This should also be clear physically. Since the undamping of the ROs can be viewed as a resonance phenomenon, one needs to have a frequency close to Ω_{RO} to excite them. However, at high injection strengths the locking range is large and so the magnitude of the detuning at the locking boundary is also large. Thus the frequency of the ROs is never reached and the resonance cannot occur. Nonetheless, as explained earlier, this route to locking must still involve a limit cycle of bounded phase.

The Class A rate equations are obtained by adiabatically eliminating the carrier equation from Eqs. (1) to (3) leading to the following pair of equations:

$$\dot{R} = \frac{P - R^2}{1 + 2R^2} R + K \cos\phi, \tag{7}$$

$$\dot{\phi} = -\Delta + \alpha \frac{P - R^2}{1 + 2R^2} - \frac{K}{R} \sin\phi. \tag{8}$$

This system has previously been considered in Refs. [5,12] but not for the features under consideration here. Note that in the free-running Class A laser, perturbations from the steady state decay exponentially and there is no intrinsic resonance that may be excited. Thus, the frequency of the Hopf bifurcation can only be associated with the injection parameters. By finding the characteristic equation, we can find this frequency

$$\Omega_H^2 = \Delta^2 - (1 + \alpha^2) N^2(R), \tag{9}$$

where $N(R) \equiv \frac{P - R^2}{1 + 2R^2}$ and R^2 is evaluated at the Hopf point. $N(R)$ is bounded with the same limits as N in the Class B case, and so as the injection strength is increased the detuning term becomes ever more prominent and for high injection strengths we recover the same result as for the Class B system, namely, that $\Omega_H^2 \approx \Delta^2$.

In fact, in the Class A system the value of R^2 is fixed at a Hopf bifurcation and is independent of the detuning and injection strength and dependent only on P and must satisfy

$$R^4 + R^2 - P/2 = 0. \tag{10}$$

To illustrate a specific example let us take $\alpha = 2$ and $P = 0.5$. We thus have $R^2 \approx 0.207$ and

$$\Omega_H^2 = \Delta^2 - 0.214. \tag{11}$$

This shows that for $P = 0.5$ we can only have a Hopf bifurcation for $|\Delta| \geqslant \sqrt{0.214}$. It also shows that the value of the detuning is crucial for determining the Hopf frequency at all injection strengths in stark contrast to the Class B system.

Figure 3 shows a locked to unlocked transition through a Hopf bifurcation. From top to bottom we see the phase evolution from (a) phase locked, through (b) unlocked with bounded phase to (c) unlocked with unbounded phase. At this injection level the angular frequency of the cycle created in the Hopf bifurcation is approximately $\Omega_H = 4.79$ and occurs at a detuning of approximately $\Delta = 4.81$ (both in units of radians per inverse photon lifetime), and so we have a close correspondence between the two. This must also hold for a Class B laser undergoing sufficiently high injection levels, in agreement with Eq. (4). Note that there is no bifurcation associated with the unbounding of the phase. An experimental transition to locking via such a Hopf bifurcation for a highly damped quantum dot device is shown in the next section.

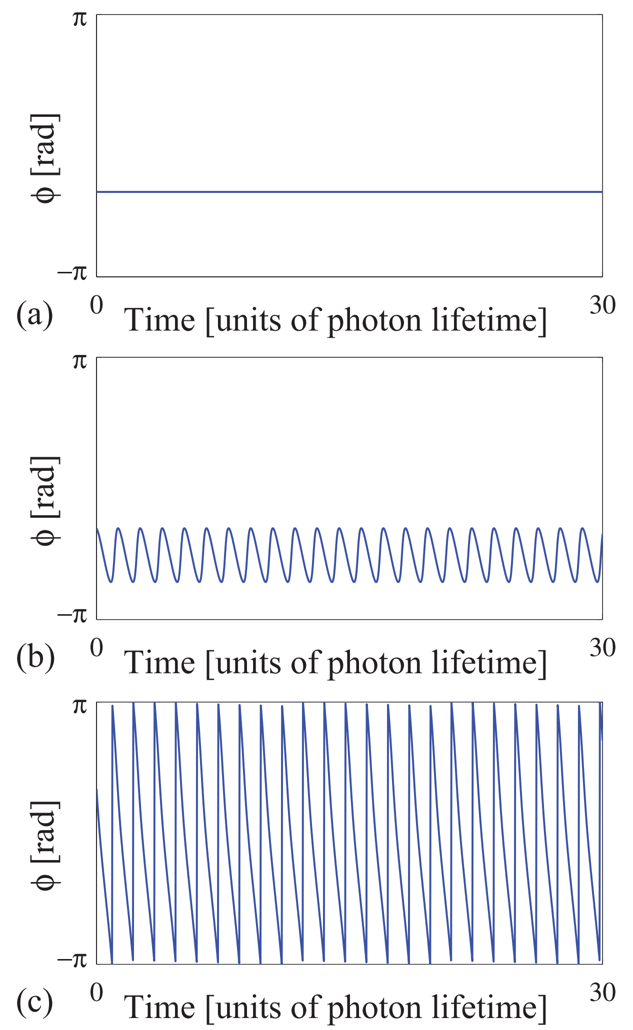

FIG. 3. (Color online) Numerical simulation of the evolution of the phase in a transition from phase locked to unlocked for a Class A laser. (a) Fixed phase corresponding to phase-locked behavior; (b) unlocked behavior with a limit cycle of a bounded phase; and (c) unlocked behavior with a limit cycle of an unbounded phase. The parameters were $K = 2$, $\alpha = 2$, $P = 0.5$, and $\Delta = 0, 4.82$, and 10, respectively.

V. EXPERIMENTAL QUANTUM DOT PHASORS

To experimentally probe a highly damped device we used a single mode distributed feedback (DFB) quantum dot laser with an InAs/InGaAs active region emitting at approximately 1.3 μm of similar construction to those used in Ref. [24]. These devices have a much higher RO damping than conventional semiconductor lasers [25–27]. This leads to several important differences when compared to quantum well and bulk lasers including a greatly increased tolerance to external optical feedback [26] and mutual coupling [24] and similarities with Class A devices when optically injected [2]. The rate equation model for quantum dot lasers should in principle be different to that used for quantum well based devices. However, our intention is to explain the observations

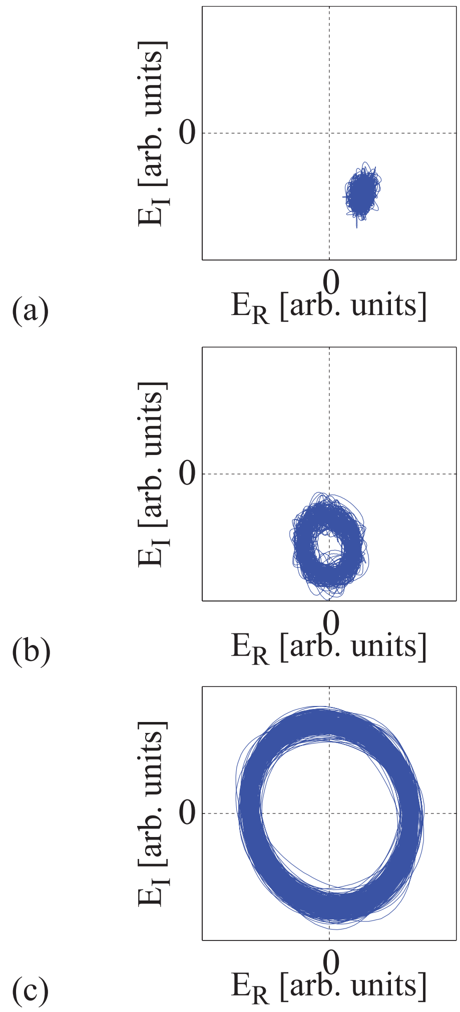

FIG. 4. (Color online) Experimental phasors for the transition from locked to unlocked behavior for a quantum dot device through a Hopf bifurcation. The device was operated at approximately 1.2 times the threshold current. The ratio of the intensity of the master laser reaching the slave to the intensity of the slave when free running was approximately 0.7. (a) Phase-locked behavior at a detuning of approximately -3 GHz; (b) unlocked behavior with a bounded phase limit cycle at a detuning of approximately 1.8 GHz; and (c) unlocked behavior with an unbounded phase limit cycle at a detuning of approximately 6 GHz.

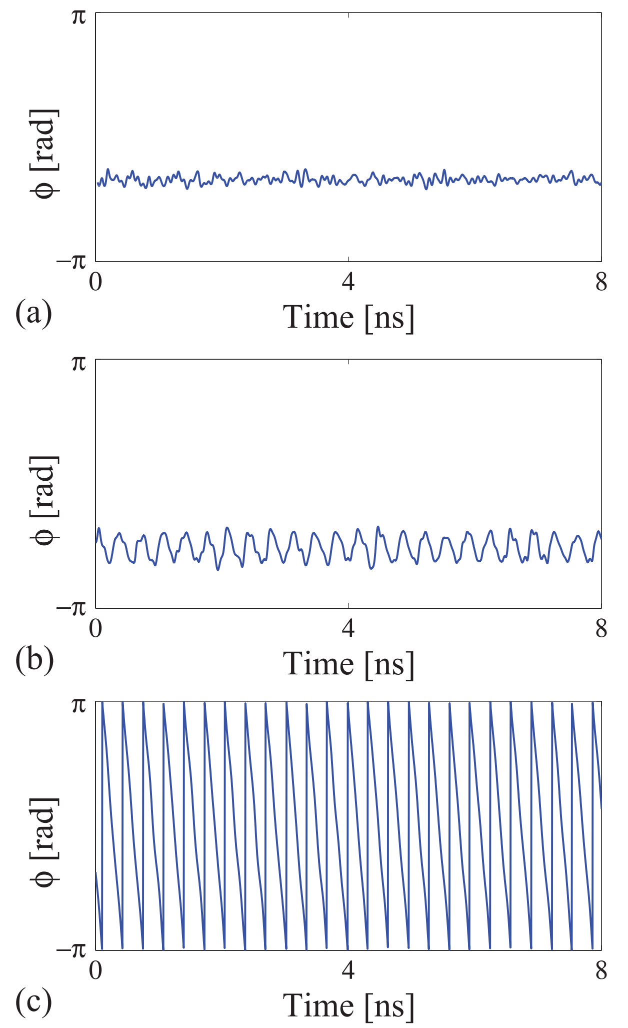

FIG. 5. (Color online) Experimental phases corresponding to the phasors in Fig. 4.

physically, and so we make use of the noted similarity between optically injected (InAs/InGaAs) quantum dot devices and optically injected Class A devices and content ourselves with qualitative comparisons of the numerical simulations and the experimental measurements.

Figure 4 shows the evolution of the phasor of a quantum dot laser over a transition from (a) phase locked to (b) unlocked with a bounded phase and finally to (c) unlocked with an unbounded phase, the same regimes as in the Class A numerical simulations in Fig. 3. The injection level is quite high here; the intensity of the light from the master laser reaching the slave was approximately 0.7 times the free-running intensity of the slave. In particular, this is much higher than the values where the locking boundaries are given by saddle-node bifurcations for both signs of the detuning; the locking for positive detuning was via Hopf for injection strengths of approximately 0.07 and greater. The bounded limit cycle is clear in Fig. 4(b). In contrast to the weak injection case the transition from bounded phase to unbounded phase does not involve any intermediate regime or any corresponding bifurcation, as already mentioned. Rather, the cycle of Fig. 4(b) simply migrates and grows in size continuously to become that of Fig. 4(c). Figure 5 shows the corresponding plots of the time series of the phase of the slave laser displaying excellent qualitative agreement with the numerical evolutions shown in Fig. 3.

Comparisons of the Hopf frequency and the detuning at various injection strengths show a good qualitative agreement with Eq. (9). The frequency of the cycle born in the Hopf bifurcation at an injection strength of 0.7 was approximately 2.8 GHz and occurred at a detuning of approximately 1.8 GHz. While these are different, they are sufficiently close that the detuning must provide a significant contribution to the Hopf frequency. At the lowest injection strength where the (positive detuning) locking boundary was of Hopf form—approximately 0.07—the frequency of the cycle created was 1.8 GHz while the detuning was approximately 0.7 GHz.

Again, these are sufficiently close that the detuning is a significant contribution. By moving to high injection levels the two can become almost equal. When the intensity of the master laser reaching the slave was approximately 2.2 times the free-running intensity of the slave, the frequency of the cycle created in the Hopf bifurcation was 6.7 GHz while the detuning was approximately 6.6 GHz, in extremely close correspondence. Thus the detuning is always a significant factor in the Hopf frequency and increasingly so as the injection strength increases, in excellent qualitative agreement with Eq. (9) and in great contrast to the Class B case where it is sometimes merely a small perturbation. This is yet another feature of the optically injected quantum dot system qualitatively similar to the Class A system [2].

VI. CONCLUSIONS

We have shown that the presence of an unlocked solution of bounded phase exists generically in optically injected lasers. The phenomenon is a direct result of the Hopf bifurcation locking mechanism and need not result from any intrinsic frequency in the laser. Theoretical considerations and simulations of rate equation models of both Class B and Class A lasers show two particular cases. For a weakly damped laser there can be a bounded cycle resulting from an excitation of the RO resonance in the system, while for a highly damped or Class A device there is no such excitation, yet a cycle of bounded phase must still arise. We derived an expression for the frequency of the Hopf bifurcation in optically injected Class A lasers and showed that the detuning must always play a significant role in the value of this frequency in contrast to the corresponding expression for Class B lasers. An experimental technique to directly resolve the phase of the slave laser in the frame of the master confirmed the existence of the phenomenon for both weakly damped devices and highly damped devices and were in excellent agreement with simulations. The phasor in a chaotic regime for the weakly damped laser displayed a combination of bounded and unbounded features allowing for a distinctive view of the regime suggesting that this type of measurement may be useful in further studies of chaos in the system.

ACKNOWLEDGMENTS

This research was enabled by the Higher Education Authority Program for Research in Third Level Institutions (2007-2011) via the INSPIRE programme, and the authors also gratefully acknowledge the support of the Science Foundation Ireland under Contract No. 07/IN.1/I929 and also through the Centre for Telecommunications Value-Chain Research (CTVR).

[1] S. Wieczorek, B. Krauskopf, T. B. Simpson, and D. Lenstra, Phys. Rep. **416**, 1 (2005).

[2] B. Kelleher, D. Goulding, S. P. Hegarty, G. Huyet, Ding-Yi Cong, A. Martinez, A. Lemaître, A. Ramdane, M. Fischer, F. Gerschütz, and J. Koeth, Opt. Lett. **34**, 440 (2009); T. Erneux, E. A. Viktorov, B. Kelleher, D. Goulding, S. P. Hegarty, and G. Huyet, *ibid.* **35**, 937 (2010); D. Goulding, S. P. Hegarty, O. Rasskazov, S. Melnik, M. Hartnett, G. Greene, J. G. McInerney, D. Rachinskii, and G. Huyet, Phys. Rev. Lett. **98**, 153903 (2007).

[3] L. Olejniczak, K. Panajotov, H. Thienpont, and M. Sciamanna, Phys. Rev. A **82**, 023807 (2010); Lukasz Olejniczak, Krassimir Panajotov, Sebastian Wieczorek, Hugo Thienpont, and Marc Sciamanna, J. Opt. Soc. Am. B **27**, 2416 (2010).

[4] B. Kelleher, C. Bonatto, G. Huyet, and S. P. Hegarty, Phys. Rev. E **83**, 026207 (2011).

[5] C. Mayol, R. Toral, C. R. Mirasso, and M. A. Natiello, Phys. Rev. A **66**, 013808 (2002).

[6] Z. George Pan, S. Jiang, M. Dagenais, R. A. Morgan, K. Kojima, M. T. Asom, R. E. Leibenguth, G. D. Guth, and M. W. Focht, Appl. Phys. Lett. **63**, 2999 (1993).

[7] I. Gatare, M. Sciamanna, J. Buesa, H. Thienpont, and K. Panajotov, Appl. Phys. Lett. **88**, 101106 (2006).

[8] A. Hurtado, A. Quirce, A. Valle, L. Pesquera, and M. J. Adams, Opt. Express **18**, 9423 (2010).

[9] W. Coomans, S. Beri, G. Van der Sande, L. Gelens, and J. Danckaert, Phys. Rev. A **81**, 033802 (2010).

[10] P. Heinricht, B. Wetzel, S. O'Brien, A. Amann, and S. Osborne, Appl. Phys. Lett. **99**, 011104 (2011).

[11] R. Adler, Proc. IRE **34**, 351 (1946).

[12] B. Kelleher, D. Goulding, G. Huyet, E. A. Viktorov, T. Erneux, and S. P. Hegarty, Phys. Rev. E **84**, 026208 (2011).

[13] A. Gavrielides, V. Kovanis, P. M. Varangis, T. Erneux, and G. Lythe, Quantum Semiclass. Opt. **9**, 785 (1997).

[14] P. A. Braza and T. Erneux, Phys. Rev. A **41**, 6470 (1990).

[15] M. K. Stephen Yeung and S. H. Strogatz, Phys. Rev. E **58**, 4421 (1998).

[16] J. Thévenin, M. Romanelli, M. Vallet, M. Brunel, and T. Erneux, Phys. Rev. Lett. **107**, 104101 (2011).

[17] B. Kelleher, D. Goulding, B. Baselga-Pascual, S. P. Hegarty, and G. Huyet, Eur. Phys. J. D **58**, 175 (2010).

[18] J. R. Tredicce, F. T. Arecchi, G. L. Lippi, and G. P. Puccioni, J. Opt. Soc. Am. B **2**, 173 (1985).

[19] A. Gavrielides, V. Kovanis, and T. Erneux, Opt. Commun. **136**, 253 (1997).

[20] Specifically we assume that $\gamma = \varepsilon\sigma$ and that $\eta = \varepsilon\eta_1$ with $\varepsilon \ll 1$. We then assume that the resulting changes in N and R from the injection-free values ($N_f = 0$ and $R_f = \sqrt{P}$) are also of this order and are $N = \varepsilon n$ and $R = R_f + \varepsilon r$. Finally, we also take $\Delta = \varepsilon\delta$ since we are concerned only with regions in or near the locking region.

[21] T. Erneux, A. Gavrielides, and V. Kovanis, Quantum Semiclass. Opt. **9**, 811 (1997).

[22] S. Wieczorek, B. Krauskopf, and D. Lenstra, Phys. Rev. Lett. **88**, 063901 (2002).

[23] B. Krauskopf, S. Wieczorek, and D. Lenstra, Appl. Phys. Lett. **77**, 1611 (2000).

[24] S. P. Hegarty, D. Goulding, B. Kelleher, G. Huyet, M.-T. Todaro, A. Salhi, A. Passaseo, and M. De Vittorio,

Opt. Lett. **32**, 3245 (2007); B. Kelleher, C. Bonatto, P. Skoda, S. P. Hegarty, and G. Huyet, Phys. Rev. E **81**, 036204 (2010).

[25] M. Kuntz, N. N. Ledentsov, D. Bimberg, A. R. Kovsh, V. M. Ustinov, A. E. Zhukov, and Yu. M. Shernyakov, Appl. Phys. Lett. **81**, 3846 (2002).

[26] D. O'Brien, S. P. Hegarty, G. Huyet, J. G. McInerney, T. Kettler, M. Laemmlin, D. Bimberg, V. M. Ustinov, A. E. Zhukov, S. S. Mikhrin, and A. R. Kovsh, Electron. Lett. **39**, 1819 (2003).

[27] T. Erneux, E. A. Viktorov, and P. Mandel, Phys. Rev. A **76**, 023819 (2007).